Global polarization of lambda hyperons in the MPD experiment at NICA energies
Глобальная поляризация лямбда-гиперонов в эксперименте MPD при энергиях NICA

D. Flusova[a,b,c,1], *P. Parfenov*[a,b], *V. Troshin*[a,b], *A. Taranenko*[a,b]

Д.С. Флусова[a,b,c,1], *П.Е. Парфенов*[a,b], *В.В. Трошин*[a,b], *А.В. Тараненко*[a,b]

[a] Joint Institute for Nuclear Research JINR, Dubna

[a] Объединенный Институт Ядерных Исследований ОИЯИ, Дубна

[b] National Research Nuclear University MEPhI, Moscow

[b] Национальный Исследовательский Ядерный Университет МИФИ, Москва

[c] National Research Tomsk Polytechnic University TPU, Tomsk

[c] Национальный исследовательский Томский политехнический университет ТПУ, Томск

Спиновая поляризация Λ-гиперонов демонстрирует анизотропное выравнимание вдоль суммарного орбитального углового момента системы столкновения, и может быть использована в качестве маркера завихренности в сильно взаимодействующей материи. В работе изучается распад $\Lambda \to p\pi^-$ для измерения глобальной поляризации в столкновениях тяжёлых ионов; применяется методика, ранее использованная коллаборацией STAR для исследования вихревой структуры образующейся среды. Подход реализован для столкновений Xe+Xe при энергии $\sqrt{s_{NN}} = 2.87$ ГэВ на нуклонную пару; события сгенерированы с помощью модели UrQMD. Полученные результаты служат базовым ориентиром для будущих экспериментальных измерений с детектором MPD.

The spin polarization of lambda hyperons exhibits an anisotropic alignment with the total orbital angular momentum of the collision system, serving as a probe for vorticity in the strongly-interacting matter. We study the lambda hyperon decay into proton-pion pair to measure global polarization in heavy-ion collisions, adopting an approach previously used by the STAR Collaboration to investigate the vortical structure of the produced medium. This method is now applied to Xe+Xe collisions at a center-of-mass energy of 2.87 GeV per nucleon pair, generated with the UrQMD model. The results provide a baseline for future experimental measurements with the MPD detector.

PACS: 25.75.-q, 25.75.Ld

[1]E-mail: dflusova@jinr.ru

Introduction

The study of the properties of strongly interacting (QCD) matter is a central goal of many experimental collaborations, including HADES(FAIR), STAR(RHIC) and NA61/SHINE(SPS). The MPD experiment in fixed-target (FXT) mode will cover energy range $\sqrt{s_{NN}}$ = 2.3–3.5 GeV, extending the MPD experiment program to lower energy [1]. The properties of QCD matter can be probed using anisotropic flow measurements, strangeness production and spin-related observables. The anisotropic flow measurements provide the information about initial geometry of the collision. On the other hand, vorticity of the medium can be probed by the global polarization measurements of produced hyperons. The high net-baryon density matter is fluid-like with small effective viscosity, and the vorticity plays important role in the evolution of the system [2].

The High Acceptance Di-Electron Spectrometer (HADES) has measured Λ-hyperons as a function of collision centrality, transverse momentum (p_T) and rapidity (y) for centrality range 0-40% at few-GeV beam energies (Au+Au at $\sqrt{s_{NN}}$ = 2.4 GeV and Ag+Ag at 2.55 GeV). The global polarization of Λ-hyperons in Ag+Ag collisions shows a strong centrality dependence, with the signal increasing towards peripheral collisions (30-40%) and approaching zero for central collisions. Within the acceptance, the polarization shows no significant variation with (p_T) or (y_{CM}) [3].

The strange Λ hyperon is so-called "self-analyzing", as its weak decay violates parity, which makes Λ ($\bar{\Lambda}$) especially suitable for global polarization measurements. The daughter proton is preferentially emitted along the spin direction of the parent Λ. In the Λ rest frame, the decay angular distribution is:

$$\frac{dN}{d\cos\theta^*} = \frac{1}{4\pi}(1 + \alpha_\Lambda P_\Lambda \cos\theta^*), \tag{1}$$

where θ^* denotes the angle of proton momentum and polarization direction in the Λ rest frame [4]; $\alpha_\Lambda = 0.732 \pm 0.014$ is a hyperon decay constant [5].

MPD in Fixed-Target mode

The fixed-target (FXT) mode of MPD covers the lower energy range with high net-baryon density in the QCD phase diagram. It complements the collider program and enables cross-checks and validation of the results with other collaborations, such as HADES and STAR. Implementation and installation of the MPD facility are in progress; accordingly, feasibility studies for a range of relativistic heavy-ion analyses are underway. The MPD–FXT program also enables direct comparison with the BM@N experiment in the same energy range. The present work focuses on the feasibility of global polarization measurements at MPD–FXT energies. For more details about MPD-FXT construction see [1].

A target is point-like and placed at $z = -85$ cm, $y = 1$ cm (see. Fig. 1), which creates asymmetry in the collision system.

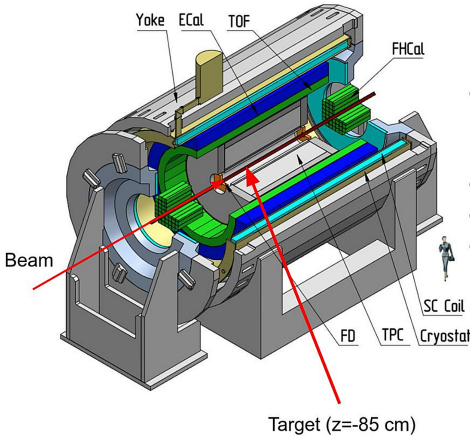
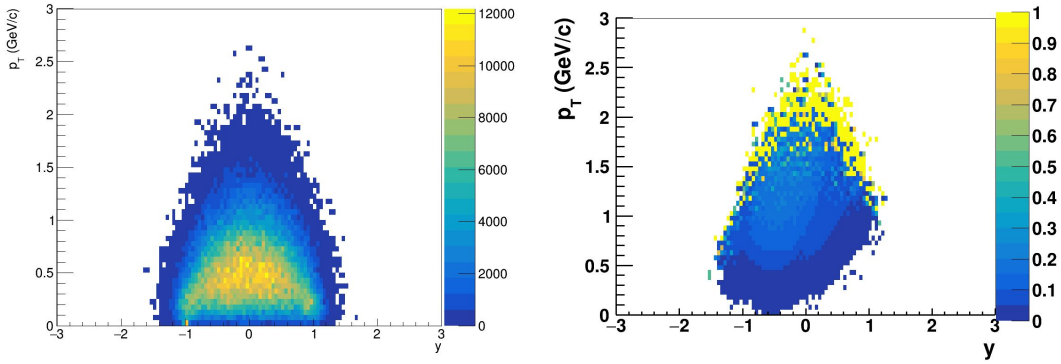


Fig. 1. MPD in Fixed-Target mode. Point-like target at $z = -85$ cm, $y = 1$ cm [1].



(a) Monte-Carlo simulated (true) Λ

(b) Reconstructed Λ
$\varepsilon(p_T, Y) = \frac{N_{\mathrm{rec}}(p_T,Y)}{N_{\mathrm{MC}}(p_T,Y)}$

Fig. 2. Transverse momentum-rapidity distribution of Λ hyperons for Monte-Carlo and reconstructed data.

FXT mode causes the assymetrical reconstruction in the transverse momentum-rapidity phase space, that leads to importance of the efficiency corrections. Figure 2(a) shows the MC generated (UrQMD) (p_T, Y) symmetric distribution of Λ-hyperons. After the full reconstruction chain, however, the efficiency becomes asymmetric and degrades toward forward rapidities. The reconstruction efficiency increases with p_T.

Dataset

Around 10 milllion events were produced with UrQMD 3.4 for Xe+Xe collisions at $\sqrt{s_{NN}} = 2.87\,\mathrm{GeV}$. To enhance statistics for global polarization studies, an "afterburner" had generated five additional Λ hyperons per event, with realistic v_1, v_2, and P_Λ signals injected into the sample. This enhancement allows statistically significant estimates without producing a huge amount of data which consumes disk storage and CPU-time.

The KFParticle–based analysis procedure is outlined in [6], with an implementation in the Particle Finder Simple (PFSimple); detailed selection cuts are provided therein. The KFParticle formalism applies a Kalman–filter treatment to neutral and charged long-lived decays, is agnostic to collider vs. FXT kinematics, and supports cascade topologies. Mother and daughter tracks are handled within the same state-vector/covariance framework, enabling consistent vertex fits, pointing-angle constraints, and decay-length significance. For each candidate the framework propagates kinematics and decay observables used in selections and efficiency corrections, including momentum p, energy E, mass m, proper decay length $c\tau$, flight distance L, and rapidity y.

The self-analyzing Λ hyperon is reconstructed via the weak decay $\Lambda \to p\pi^-$ [6]. Λ candidates are formed by combining each negatively charged track (π^- candidate) with each positively charged track (p candidate), followed by topological and kinematic selections applied to the reconstructed decay vertex and daughter tracks. Centrality selection is performed at the simulation level using the impact parameter. Track quality cuts require, at the minimum, $N_{\text{hits}} > 10$ and the appropriate charge assignment for proton and pion candidates.

The following topological selections are applied to Λ candidates: $\chi^2(p) > 60$ and $\chi^2(\pi^-) > 200$ reject tracks originating from the primary vertex (selection of daughter tracks); $DCA < 1$ cm is small distance of the closest approach between daughter tracks at their mutual closest point; $L > 2.5$ cm is decay length cut; removes very short-lived (near-primary) candidates; $L/dL > 20$ is decay-length significance; requires the secondary vertex to be well separated from the primary vertex in units of its uncertainty; $\chi^2_{geo} < 100$ is geometric fit quality of the common secondary vertex; $\chi^2_{topo} < 100$ is topological fit quality.

Invariant-Mass fit method

The common invariant-mass method is widely used for collective flow analysis and for global polarization extraction. It can be assumed that the physics observable (e.g., v_n or P_Λ) is independent of the invariant mass m_{inv}, whereas the signal-to-background ratio varies with m_{inv}. By fitting the measured observable in the signal window as a mixture of signal and background across m_{inv}, one obtains an unbiased estimate of the signal value from data [7].

$$P^{SB}(m_{inv}) = P^S \frac{N^S(m_{inv})}{N^{SB}(m_{inv})} + P^B \frac{N^B(m_{inv})}{N^{SB}(m_{inv})}, \tag{3}$$

where terms N^S/N^{SB} and N^B/N^{SB} are results from previously done fits; P^{SB}, P^S and P^B are relevant parameters from the second distribution. The P^S is required value as fitting parameter.

The STAR Collaboration [8] demonstrated that in a magnetic field the daughter tracks follow helical trajectories; from "left" decays paths are deflected and "right" decays paths are crossed in transverse plane, producing

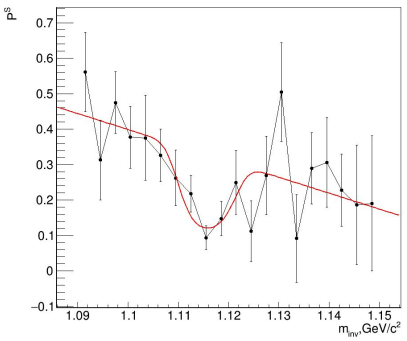
an azimuthally nonuniform acceptance. As a result, a sinusoidal contribution appears $\langle \sin(\Psi_1 - \phi_\Lambda) \rangle \neq 0$ in Eq. (4).

The residual bias can be monitored via the relation $\langle \sin(\Psi_1 - \phi_\Lambda) \rangle$ and, if nonzero, subtracted:

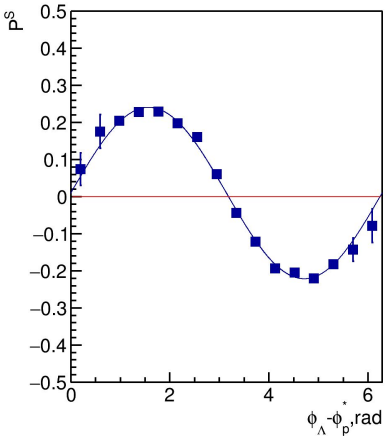
$$\frac{8}{\pi \alpha_\Lambda} \frac{1}{R^{(1)}_{EP}} \langle \sin(\Psi_1 - \phi^*_p) \rangle^{sig} = \bar{P}_\Lambda + c \sin(\phi_\Lambda - \phi^*_p), \tag{4}$$

where c quantifies the coupling of directed flow v_1 to the detector acceptance. The acceptance asymmetry is corrected independently in forward ($y > 0$) and backward ($y < 0$) rapidities, and the two estimates are then combined as a weighted average $\bar{P}_\Lambda = \frac{1}{2}(\bar{P}_\Lambda(y > 0) + \bar{P}_\Lambda(y < 0))$ [8].

The Figure 3 demonstrates the generalized invariant-mass fit procedure; in such method values under investigation do not depend on invariant-mass value, hence it is possible to use the distribution for clearer signal extraction with (4) and (3) equations. The final signal distribution in the Fig. 3(b) is shown. The acceptance asymmetry is corrected with weighting over polarization value for forward and backward rapidities.



(a) Signal extraction (P^{SB}): Fitting of the global polarization as a function of the invariant mass.



(b) Fitting of the global polarization in bins of the azimuthal angle difference between the Λ hyperon and the daughter proton (in the Λ rest frame).

Fig. 3. Application of the generalized invariant-mass fitting method to the measurement of global polarization of Λ-hyperons

Analysis

The analysis uses the QnTools framework, which is based on the flow–vector formalism. For each particle, the unit vector $\mathbf{u}_n \equiv e^{in\phi}$ is constructed from its azimuthal angle ϕ in the transverse plane. The event flow vector

is then $\mathbf{Q}_n \equiv \sum_i w_i\, e^{in\phi_i}$ where w_i are per-track weights [9, 10]. In practice, QnTools performs recentering and flattening of $\mathbf{Q}_n$ to correct detector non-uniformities, and uses subevents to estimate the event plane resolution R_n [11].

To suppress non-flow contribution and avoid autocauto-correlations, the event plane is estimated from independent subevents. The FHCal has a modular structure composed of three concentric rings around the beam axis, which can be utilized as three sub-events. Additional subevents are constructed from charged tracks within $-1.0 < y < -0.6$ rapidity window. For each subevent $\mathbf{Q}_n$ was calculated, then correction factor from three subevent correlations (3S resolution) is:

$$R_1^{F1(F3,Tp)} = \frac{\sqrt{\langle Q_1^{F1} Q_1^{F3}\rangle \langle Q_1^{F1} Q_1^{Tp}\rangle}}{\sqrt{\langle Q_1^{F3} Q_1^{Tp}\rangle}}, \tag{5}$$

where Q_1^{F1} and Q_1^{F2} are calculated from modules 1 and 2 of the FHCal, respectively, while Q_1^{Tp} is derived from the charged-particle multiplicity in the TPC detector. The final correction factors are shown in Fig. 4. The correction factors vary since they are computed for different sub-events, but they still follow the general trend.

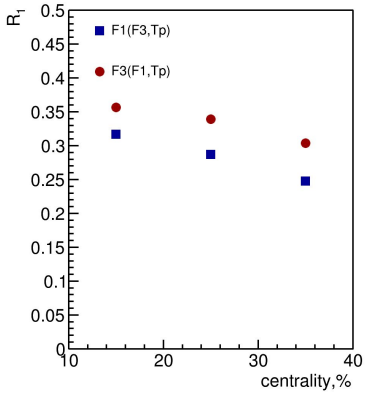


Fig. 4. The resolution correction factor relative to centrality classes for MPD-FXT, $Xe + Xe$ @ 2.87 GeV.

For the measurement of global polarization using QnTools, the xy/yx components of the $\mathbf{uQ}$ vector correlations are utilized: $P = \frac{8}{\pi\alpha} \frac{\langle u_1 Q_1^{F1}\rangle}{R_1^{F1}}$, where R_1^{F1} is a correction factor, see. Eq. 5.

Results

Figure 5 shows the global polarization of Λ hyperons as a function of rapidity y in Xe+Xe collisions at $\sqrt{s_{NN}} = 2.87\,\text{GeV}$. The MC true signal is drawn as a red line, the reconstruction with the common invariant–mass method appears as green markers, and the generalized invariant–mass method (as used by STAR [8]) is shown as blue markers. The

common invariant–mass fit reproduces the v_1 trend and deviates significantly from the MC true signal. v_1 induces a non–zero correlation between the Λ azimuth and the event plane. The generalized invariant–mass method minimizes this effect. The acceptance correction was applied, calculated as $\frac{4}{\pi}\langle\sin(\theta_p^*)\rangle$, where θ_p^* is the polar angle of the proton in the Λ rest frame [12]. However, current discrepancy is still high. Therefore, the disagreement is under active investigation.

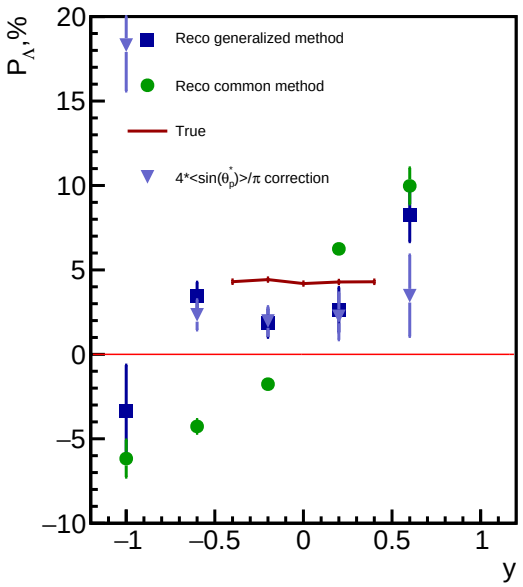


Fig. 5. Global polarization of Λ-hyperons: red line is MC (true) data; green points are the common invariant-mass fit; blue markers are the generalized invariant-mass fit; purple markers are the generalized invariant-mass fit with acceptance correction.

Conclusion

The simulation based feasibility study of global polarization of Λ hyperons has been done for Xe+Xe collisions at $\sqrt{s_{NN}} = 2.87$ GeV. It is also planned to provide same analysis for Xe+W collisions system and get predictions for the first results from the MPD-FXT configuration.

The reconstruction chain was implemented with MPDROOT and candidates selection via the KFParticle framework. The dataset was produced with UrQMD 3.4 generator and then realistic v_1, v_2 and P_Λ have been added to data. Additional production of Λ hyperons (up to 5 additional Λ per event) allowed to get clear signals. For global polarization analysis the invariant fit method was used: the common one gives additional non-polarization correlation, the generalized method reduces this effect. However, a noticeable discrepancy with respect to the MC true signal remains. There are additional factors that were not taken into account: possible impact from enhancement production and other systematic effects coming from reconstruction procedure.

Asymmetric reconstruction efficiency particularly at forward rapidity affects the measurement precision. Results were corrected with weighting for forward ($y > 0$) and backward ($y < 0$) rapidities. Next analysis will include recentering/flattening tuning.

The work was funded by the Ministry of Science and Higher Education of the Russian Federation, Project "Fundamental and applied research at the NICA (JINR) megascience experimental complex"" FSWU-2025-0014

REFERENCES

1. *Parfenov P.E., Mamaev M.V., Taranenko A.V.* // Physics of Particles and Nuclei. 2025. Vol. 56, no. 3. P. 921–927.

2. *Becattini F., Karpenko I., Lisa M.A., Upsal I., Voloshin S.A.* // Physical Review C. 2017. V. 95, no. 5. P. 054902. Publisher: American Physical Society.

3. *Abou Yassine R., Adamczewski-Musch J., Asal C., et al.*. // Physics Letters B. 2022. V. 835. P. 137506.

4. *Kornas F.J.* // The XVIII International Conference on Strangeness in Quark Matter (SQM 2019) / Ed. by Domenico Elia, Giuseppe E. Bruno, Pietro Colangelo, Leonardo Cosmai. Cham : Springer International Publishing, 2020. P. 435–439.

5. *Zyla P., Barnett R., Beringer J., et al.*. // Progress of Theoretical and Experimental Physics. 2020. V. 2020, no. 8. P. 083C01.

6. *Lubynets O., Selyuzhenkov I., Klochkov V.* // Particles. 2021. Vol. 4, no. 2. P. 288–295. Publisher: Multidisciplinary Digital Publishing Institute.

7. *Troshin V.V.* // Physics of Particles and Nuclei. 2025. V. 56. P. 903–908. ADS Bibcode: 2025PPN....56..903T.

8. *Abdallah M., Aboona B., Adam J., et al.*. // Physical Review C. 2021. V. 104, no. 6. P. L061901. Publisher: American Physical Society.

9. *Poskanzer A.M., Voloshin S.A.* // Physical Review C. 1998. V. 58, no. 3. P. 1671–1678. Publisher: American Physical Society.

10. *Bilandzic A., Snellings R., Voloshin S.* // Physical Review C. 2011. V. 83, no. 4. P. 044913. Publisher: American Physical Society.

11. *Mamaev M., Taranenko A.* // Particles. 2023. Vol. 6, no. 2. P. 622–637. Publisher: Multidisciplinary Digital Publishing Institute.

12. *Abelev B., Aggarwal M.M., Ahammed Z.* // Phys. Rev. C. 2007. V. 76. P. 024915.